Effect of Medium for Enhanced Nanosensing: DDA Theory vs Experimental Studies of Ag Nanoparticle Assemblies

ARTICLE *in* THE JOURNAL OF PHYSICAL CHEMISTRY C · JANUARY 2010

Impact Factor: 4.77 · DOI: 10.1021/jp907991w

2 AUTHORS, INCLUDING:

Shiliang Wang
Suffield Research Centre
39 PUBLICATIONS **340** CITATIONS

Effect of Medium for Enhanced Nanosensing: DDA Theory vs Experimental Studies of Ag Nanoparticle Assemblies

Shiliang Wang and David B. Pedersen*

Defence R&D Canada, Suffield, Suffield, Alberta T1A 0R9, Canada

Received: August 18, 2009; Revised Manuscript Received: November 30, 2009

Gas-phase deposition has been used to assemble two-dimensional ensembles of strongly coupled 3.0 ± 0.5 nm diameter naked Ag nanoparticles. The coupling mechanism is found to be complex suggesting dipole−dipole coupling at relatively long distances but wave function overlap at center-to-center distances less than 25 nm. The coupled nanoparticles are found to display enhanced sensitivity to changes in the refractive index of the medium, relative to the isolated particle system, and the experiments confirm theoretical predictions of the enhancement effect. For the Ag nanoparticles considered, the enhancement effect is interesting as the coupling energy between particles is found to be remarkably insensitive to the medium and changing the surrounding material from air to hexane has no noticeable effect on this energy. At the same time, changing the medium from air to hexane always manifests a 0.14 eV shift (as for the individual nanoparticle) independent of interparticle coupling and distance. In noncoupled systems the SPR appears at shorter wavelength where the 0.14 eV energy amounts to a relatively small shift in the peak position wavelength. In coupled systems, however, the SPR is positioned at relatively long wavelengths and 0.14 eV is a large shift in wavelength units. As the enhancement is the wavelength change per refractive index unit, more coupled systems yield higher enhancement. The fact that enhanced sensitivity is observed in two-dimensional assemblies of nanoparticles demonstrates that the effect is not restricted to nanoparticle dimers, specifically, as previously thought. The results suggest that any geometric arrangement of closely spaced nanoparticles that generates strong interparticle coupling interactions can form the basis of SPR-based sensor elements with the benefit of near-field enhanced sensitivity.

Introduction

The development of assemblies of metal nanoparticles as sensor elements requires an understanding of the impact of interparticle coupling on the sensitivity of the optical response to changes in the local environment. Due to the high polarizability of the free electron gas, dipole−dipole interactions between neighboring metal nanoparticles are strong and span distances of 100 nm or more. In nanoparticle dimers, this coupling has been shown to effect a shift of more than 140 nm in the peak absorbance of the surface plasmon resonance (SPR).[1,2] In two-dimensional nanoparticle assemblies, shifts of more than 400 nm have been reported.[3] The magnitude of these shifts testifies to the importance of interparticle coupling on the optical properties of assemblies of metal nanoparticles.

Schatz and van Duyne have demonstrated that theory based on the discrete dipole approximation (DDA theory) captures most of the interparticle coupling effect on the optical properties of nanoparticle ensembles.[4−8] The effect of changes in the spacing between particles and changes to the geometry of the ensemble can be predicted with this approach, and experimental evidence supports the validity of the theory. The impact of interparticle coupling on sensing capability, however, has received little attention. Recently, Jain and El-Sayed have focused attention on this more practical aspect of nanoparticle-based sensors and the possibility of utilizing interparticle coupling to enhance sensitivity.[9] Using DDA theory, they conclude that the sensitivity of the SPR of a coupled nanoparticle pair, to changes in the refractive index of the surrounding medium, is enhanced relative to the sensitivity of isolated particles to similar changes. They find that the sensitivity increases from 77 to 172 nm per refractive index unit (RIU^{-1}) as the separation between a pair of naked 40 nm diameter gold particles is decreased from the noncoupled state to near-touching. Experiments by the Quidant group have used ebeam lithography to demonstrate this kind of enhancement in nanoparticle dimers.[10,11] The data do not, unfortunately, lend themselves well to direct quantitative comparison with the predictions of Jain and El-Sayed and experiments more amenable to validating the theory are desirable.

Fashioning naked nanoparticle dimers with well-defined interparticle separations, that can be placed in a variety of media with different refractive indices, is challenging work and effectively restricted to the ebeam methods. The ebeam approach is relatively costly and restricted to resolution limits of 10 nm. To expand the scope and explore enhancement effects below the 10 nm limit, other approaches to fabricating nanodimensioned devices that exploit interparticle coupling effects are required. Gas-phase deposition is one approach where assemblies of naked metal nanoparticles can be made in which interparticle separations are well-defined. Recently, we demonstrated controlled assembly of two-dimensional ensembles of silver nanoparticles in which the spacing between particles could be systematically varied.[3,12] When the spacing is relatively large the interparticle coupling is minimal and the optical properties approach those characteristic of isolated nanoparticles. With decreased spacing, the properties change from this non-coupled situation to a highly coupled one, which implies a substantial

* To whom correspondence should be addressed: E-mail: david.pedersen@drdc-rddc.gc.ca.

10.1021/jp907991w Published 2010 by the American Chemical Society
Published on Web 01/07/2010

change in the extent of near-field interactions between nanoparticles. The near-field effect is substantial and quadrupolar absorbances could be observed even in small (≤10 nm) nanoparticles when internal reflection spectroscopy was utilized.[12,13] The ability to control the extent of near-field coupling between naked nanoparticles makes these nanoparticle assemblies attractive as a means of testing predictions of theory on the effects of such coupling on the SPR of nanoparticles.[9]

In light of these facts, our nanoparticles are well suited for testing the medium effect on interparticle coupling, as predicted by Jain and El-Sayed, and to explore whether such effects are observable in two-dimensional assemblies or restricted to nanoparticle dimer configurations, exclusively. In the present work, we measure the response of the SPR of coupled nanoparticle assemblies to changes in medium refractive index and compare these results directly with DDA theory. The enhanced sensitivity predicted by Jain and El-Sayed is observed which strongly supports the validity of the theoretical predictions.

Experimental Section

To prepare assemblies of silver nanoparticles, we employed a system that generates gas-phase nanoparticles in a vacuum environment and deposits these onto substrates. Ag nanoparticles were generated in the gas phase using an aggregation-type source (Mantis Nanogen) as discussed elsewhere.[3,14,13] Briefly, voltage (200−400 V, 200−300 mA) applied between an anode cap and a metal target, in the presence of a few milliTorr of Ar, sustained a plasma inside the region capped by the anode. Ar was introduced at a rate of 50 sccm (MKS 1179A mass flow controller) through a shower-head inlet directed at the anode cap and positioned immediately in front of the anode cap. The Ar gas flow was augmented with a 10 sccm flow (MKS 1179A mass flow controller) of He which was introduced into the aggregation zone through a second gas inlet. Condensation of the plasma gas began once the plasma gas exited the plasma region, through a hole in the anode cap, and entered the first aggregation zone. The gas then expanded into the second aggregation zone, which was evacuated by a 500 L s^{-1} turbo pump (Varian V-550). The nanoparticles thus generated passed through an orifice into the sample chamber where a pressure of $<10^{-4}$ Torr was maintained during deposition by a 300 L s^{-1} turbo pump (Varian TV-301). The nanoparticles were deposited onto microscope slides (Fisher Premium) positioned in the nanoparticle beam path. From scanning tunneling microscope images of the nanoparticles deposited onto highly ordered pyrolytic graphite, the diameter of the particles used in this work was found to be 3.0 ± 0.5 nm in diameter.[3] As discussed in a previous publication,[3] because the nanoparticles are negatively charged during the deposition process, Coulomb repulsion minimizes the amount of particle aggregation and coalescence that occurs. Accordingly, as the deposition proceeds the average distance between particles steadily decreases, interparticle coupling steadily increases, and the nanoparticles form monodispersed, two-dimensional assemblies.

To monitor optical properties during deposition, light from a halogen−deuterium lamp (Mikropak DH-2000) was directed into the sample chamber through an optic fiber, passed through a collimating lens, through the microscope slide, and out of the sample chamber through a quartz window.[14] The reflected light was then collected by a second collimating lens and focused into another optic fiber which carried the light to the CCD array spectrometer (Ocean Optics-SD2000). The spectrometer was set to acquire spectra every 2−3 s during deposition so that spectra of the nanoparticles could be acquired in real time, as they were being deposited.

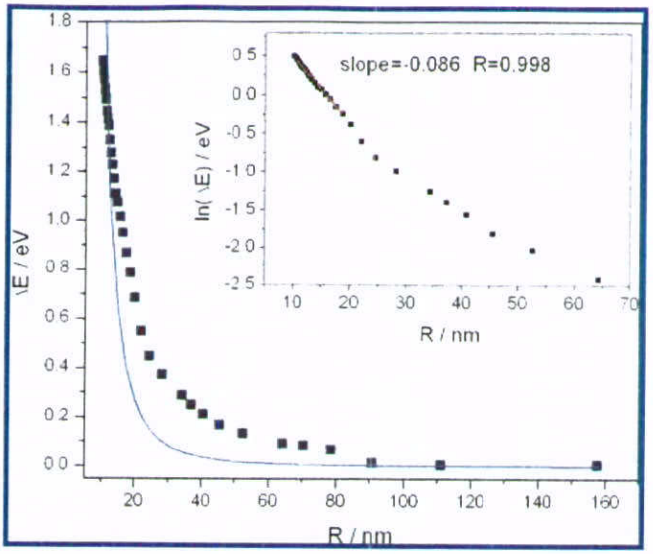

Figure 1. Shift in the SPR peak position of 3.0 ± 0.5 nm diameter Ag nanoparticles as a function of the interparticle separation. The data were acquired in situ during the deposition process. The blue line is a fit of the experimental results assuming that the SPR peak position scales as R^{-3}, where R is the interparticle (center-to-center) separation. From AFM imaging, the precision is estimated to be $R \pm 20\%$, which reflects the natural variation in interparticle separation during the deposition. The inset is a semilog plot of the same data. A linear fit is shown for the shortest distance data in the inset as a red line.

Results

Interparticle coupling effects on the optical properties of the nanoparticle assemblies are clearly evident during the deposition process. The steady shift of the SPR to longer wavelengths, as seen in Figure 1, is characteristic of increased interparticle coupling as interparticle separation is decreased.[3,13]

The absence of aggregation and coalescence during the deposition was verified using SEM and AFM images, as described elsewhere.[3,14] Imaging was also used to determine the spacing between individual nanoparticles plotted in Figure 1. Although the smooth trend observed contrasts some literature where behavior is more complicated,[15] the steady shift to longer wavelengths is expected of the 3.0 ± 0.5 nm diameter particles because they are small. Blue shifts caused by phase retardation effects are negligible for small nanoparticles because only nearest neighbor coupling is important. The SPR peak position is a smooth near-exponential function of interparticle separation accordingly.[2,16] Within the dipole−dipole coupling model, the data should vary with R^{-3}, shown as a blue line in Figure 1.

Because nearest neighbor interactions are dominant, the optical properties of the nanoparticle films are expected to mirror those predicted by Jain and El-Sayed for an isolated pair of nanoparticles. There is no evidence of long-range order in the nanoparticle assemblies so the probability of several plasmon resonance modes with different polarization behaviors is minimal.[9,17] The randomness of the deposition process coupled with the radial symmetry of the Coulomb repulsion that drives the self-assembly process appears to minimize long-range order and associated effects. The dominance of nearest-neighbor interaction is also apparent in Figure 1 where the surface plasmon resonance peak position varies smoothly as a well-behaved function of R. The naked nanoparticle films therefore constitute a suitable experimental analogue of the nanoparticle dimer model used by Jain and El-Sayed and are thus useful for testing the theoretical results.

In order to explore the impact of interparticle coupling on the sensitivity of the SPR to changes in the refractive index of

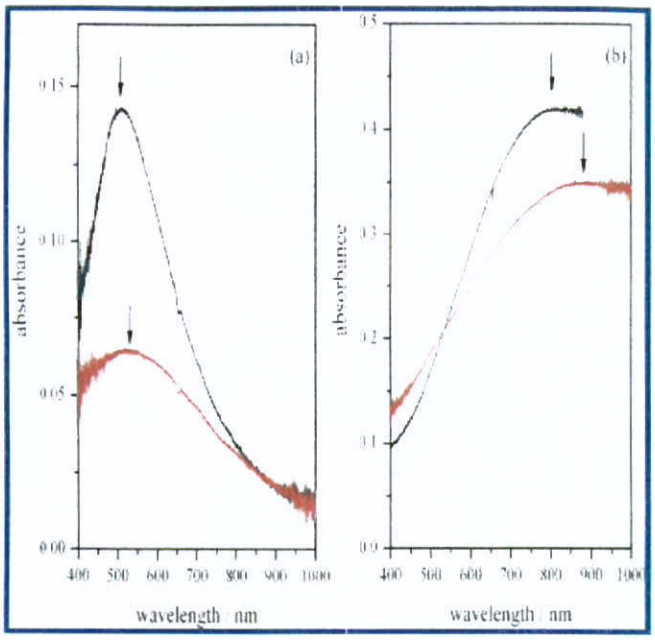

Figure 2. Absorption spectra of Ag nanoparticle films as prepared (black) and after immersion in hexane (red). (a) A relatively low density film. (b) A relatively high density nanoparticle film. The SPR peak positions are marked for each sample (see text for details).

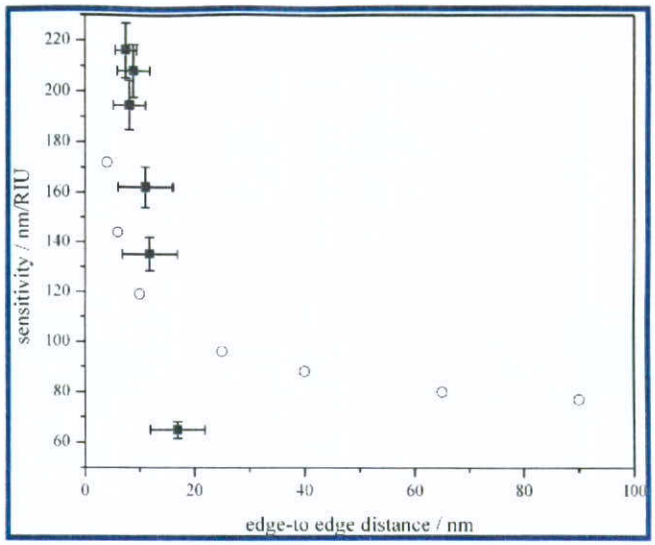

Figure 3. Experimental (squares) results showing the sensitivity of the SPR shift as a function of interparticle (edge-to-edge) separation are compared with the DDA theory results of Jain and El-Sayed (°). Although the DDA results are calculated for 40 nm diameter Au nanoparticles, the predicted trend in the data compares well with the experimental data for 3 nm diameter Ag nanoparticles. The error bars reflect the error in the AFM-determined edge-to-edge distance and the precision with which the positions of the broad SPR absorbances were determined. See text for details.

the medium, nanoparticle films were removed from vacuum and placed in ambient air and then hexane. In ambient air, both oxidation and uptake of small amounts of atmospheric water occur and a small shift (1−10 nm) in the SPR peak position to longer wavelengths was observed. After 5 min in air (refractive index of 1.00) the SPR peak position was stable. The samples were then immersed in hexane, which has a refractive index of 1.37, the optical spectra acquired, and the shift in the SPR from its value in air determined. Nonpolar solvents like hexane cause minimal restructuring of the nanoparticle assemblies, as determined via comparison of AFM images taken before and after immersion in hexane. Furthermore, the SPR peak position returned to its pre-exposed position when samples wetted with hexane were subsequently dried at room temperature under vacuum. The shift in SPR position observed upon immersion in hexane is therefore reversible and results from the change in refractive index of the medium, specifically. The type of shift observed is illustrated in Figure 2 where UV−vis absorbance spectra of two nanoparticle films are shown in air and in hexane.

The suppression in the extinction of the nanoparticle array is expected and reported previously.[18] The shifts shown are 80 and 25 nm for the high and low density nanoparticle films, respectively. These translate to 216 and 68 nm RIU^{-1}, respectively, which are the values plotted in Figure 3 below.

Discussion

The coupling effect on the SPR peak position, illustrated by the data shown in Figure 1, is typically interpreted in terms of the dipolar coupling mechanisms that constitute the basis of Förster energy transfer theory.[5,19,20] Accordingly, an equation assuming the shift in the SPR position is proportional to R^{-3}, where R is the center-to-center distance, has been fit to the data. As seen, the fit is not accurate and there are significant deviations suggesting that the coupling mechanism is not exclusively dipolar in nature. At relatively short distances, wave function overlap between neighboring nanoparticles is expected to contribute to the coupling. Analogous to Dexter energy transfer,[21] such coupling is expected to be an exponential function of R. To explore the importance of overlap-associated coupling, a plot of the log of the shift in the plasmon resonance frequency (expressed in eV) versus the center-to-center distance (R) between particles is shown in the inset in Figure 1. At relatively short distances, less than ~25 nm, the plot is remarkably linear and the coupling energy is clearly an exponential function of R. The results strongly indicate the prevalence of wave function overlap (i.e., Dexter) type coupling at relatively short interparticle separations. The significant deviation from the exponential relationship evident at longer distances is consistent with loss of overlap of the wave functions on neighboring particles, which rapidly becomes ineffective at longer distances. The changing trend in the data therefore reflects an evolution of the interparticle coupling mechanism from a power-type law, characteristic of dipole−dipole interaction,[20] to an exponential relationship characteristic of wave function overlap (i.e., Dexter-type electronic energy transfer)[21] as interparticle separation is decreased. Such evolutions of coupling have been discussed by Bagchi.[20,22] For deposition curves like Figure 1, measuring the coupling at longer distances is complicated by the fact that interparticle distances change extremely rapidly as a function of deposition time and because the low particle density gives weak absorbance. Accordingly, only a few data points are available at distances greater than 60 nm. Furthermore, the deviation about the average center-to-center distance R is larger at these distances, which has the effect of shifting the SPR to longer wavelengths than expected. At the earliest deposition times the SPR peak position can be fit with a R^{-3} dependence, as expected of a dipolar coupling mechanism. At distances between 60 and 20 nm the R^3 fit is not accurate suggesting multiple coupling mechanisms. At shorter distances, however, the SPR peak position is clearly an exponential function of R suggesting the coupling mechanism is dominated by wave function overlap.

In Figure 2, the effect of changing the medium from air to hexane on the SPR peak position is shown for low and high density nanoparticle films. The sensitivity of the higher density

film to changes in the medium refractive index (80 nm shift) is seen to be much higher than the sensitivity of the lower density film (25 nm shift). This enhanced sensitivity has been described by Jain and El-Sayed for the case of gold nanoparticle dimers.[9] For identical particles, coupling enhances the sensitivity relative to the isolated particle situation. These experimental data effectively demonstrate an enhanced sensitivity similar to that predicted by Jain and El-Sayed. To demonstrate the magnitude of the effect, in Figure 3 a plot of the sensitivity of the SPR peak position, to changes in medium refractive index, is shown as a function of the distance between nanoparticles in the assemblies.

For comparison the experimental results are compared directly with the DDA predictions of Jain and El-Sayed. The overall agreement is relatively good. Clearly, the sensitivity (expressed as shift in the SPR wavelength over the unit change in refractive index[9]) increases dramatically as the interparticle center-to-center distance decreases. The experimental results confirm the predicted enhancement in sensitivity effected by interparticle coupling. Fundamentally, however, there are some essential differences between the two systems that are expected to cause the experimental and theoretical results to differ. First, the Ag nanoparticles used in the experiments are smaller in diameter. According to theory, changes in medium should manifest a smaller shift in the SPR band position for smaller particles than for larger diameter particles.[9] Second, the optical properties of the Ag metal used experimentally and the Au considered by Jain and El-Sayed are significantly different.[23] The free electron gas is more polarizable in Ag and coupling effects are expected to be larger. Third, interparticle coupling effects are expected to be stronger in the experimental assemblies than in the dimer case considered by DDA due to the delocalization of the free electron gas in two dimensions.[3] Although all three effects are expected, it is clear from Figure 3 that their combined impact is secondary to the prominent effect of interparticle coupling and the associated enhancement in sensitivity to the medium refractive index. This effect is the dominant trend in both sets of results.

There are two obvious mechanisms by which the medium can manifest the enhanced sensitivity effect observed. The first stems from the sensitivity of the SPR to changes in the refractive index of the medium. In absence of any interparticle coupling, (i.e., individual particles) the SPR peak position is well-known to be a near-linear function of the refractive index.[24] The second, is thought to stem from the medium effect on nanoparticle polarizability.[9] As the refractive index of the medium increases the restoring force between the nanoparticle core and the free electron gas effectively decreases. The nanoparticle is therefore more polarizable in media with higher dielectric constants and stronger dipole−dipole coupling results which would manifest a larger shift in the SPR peak position. To understand the relative importance of the two effects, the change in the interparticle coupling energy has been determined as a function of the interparticle center-to-center distance. The coupling energy is equal to the SPR peak position for the isolated particle (expressed in eV) minus the SPR peak position of the coupled particle. The experimental SPR energy of isolated Ag nanoparticles in air on glass substrates in this study is 3.31 eV (375 nm). For hexane, our previous work shows 10 nm Ag nanoparticles in water (which has a refractive index comparable to that of hexane) have SPR peaks near 3.14 eV (395 nm).[25] The corresponding shift of individual Ag nanoparticles on glass will be smaller and we can estimate an upper limit of 0.17 eV in going from air to hexane. The coupling energies calculated are shown in Figure 4.

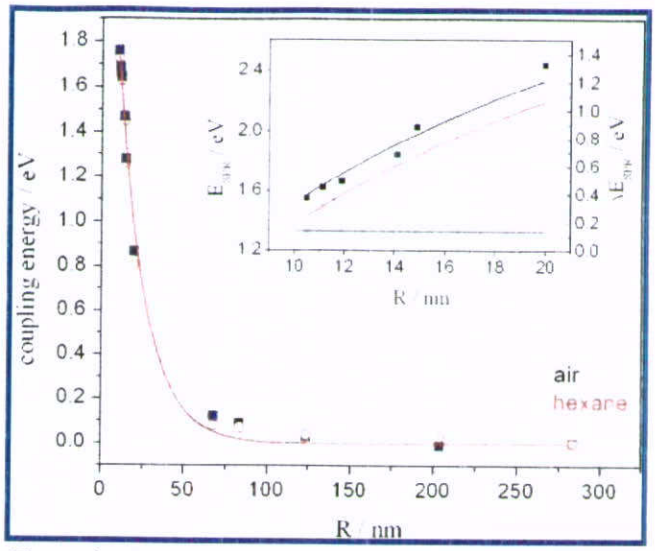

Figure 4. Coupling energy as a function of the center-to-center interparticle separation. At distances longer than 60 nm the data correspond to the coupling energies between two 40 nm Ag nanoparticles determined using DDA theory. The other points correspond to experimental measurements of the optical spectra of assemblies of 3.0 ± 0.5 nm diameter Ag nanoparticles. Data are shown for both hexane and air media. In the inset, the SPR peak positions (in eV) are shown as a function of the center-to-center distance for hexane and air media. The difference between these two (×) is also shown. The solid lines are exponential fits shown as a guide to the eye. See text for details.

Both experimental and DDA results are shown. The latter have been calculated for 40 nm diameter Ag nanoparticles using the DDSCAT 6.0 program of Draine and Flatau.[26,27] Analogous calculations for 3 nm diameter nanoparticles are too computationally demanding for the equipment and patience available. Within the estimated error, the DDA theory predicts no significant change in the coupling energy at interparticle distances greater than 70 nm. This result is consistent with Figure 1 and with the fact that distances longer than 70 nm are approaching the asymptotic limit of dipolar (i.e., Förster) type coupling.[20,22] At distances below 50 nm, the coupling energy increases dramatically. Interestingly, analogous results shown for both hexane and air in Figure 4 are seen to be equivalent within error. This is more clear in the inset where the SPR peak position is plotted as a function of R for both hexane and air. The two data sets are surprisingly parallel, indicating that the shift in SPR energy in going from air to hexane is independent of R and therefore independent of coupling. Notice that in Figure 2 the 25 and 80 nm shifts observed in the weakly (panel a) and strongly (panel b) coupled films, respectively, correspond to equivalent energy changes of 0.14 eV (i.e., the spacing between parallel lines in the inset of Figure 4). Remarkably, both experiment and DDA demonstrate a near-absence of dependence of the coupling energy on the medium.

The polarizability model, proposed above, provides one possible explanation of the insensitivity of the Ag nanoparticles to changing the medium from air to hexane. From the Lorentz−Lorenz equation, the sensitivity of the polarizability to the medium is given by

$$\alpha = 3V\frac{\varepsilon_{Ag} - \varepsilon_m}{\varepsilon_{Ag} + 2\varepsilon_m} \quad (1)$$

where V is the particle volume, ε_m and ε_{Ag} are the dielectric constants of the medium and the Ag nanoparticle, respectively. From eq 1 the magnitude of the medium effect on α is seen to depend on the relative magnitudes of ε_{Ag} and ε_m. At wavelengths longer than ~600 nm the effect of changing ε_m is minimal because the magnitude of ε_{Ag} is large.[28] Accordingly, the polarizabilty of the free electron gas in the coupled Ag nanoparticle system, where the plasmon resonance occurs at long wavelengths, is relatively unaffected by the medium. The polarizability model therefore provides an explanation for the constancy of the coupling energy observed for Ag nanoparticles in the different media.

Since changing the medium has no effect on the coupling energy in the Ag nanoparticle ensembles, the shifts observed in going from air to hexane must stem from the refractive index effect. In the Ag nanoparticle ensembles, the effect amounts to a 0.14 eV shift that is coupling independent and the same for all nanoparticle ensembles considered. Relating wavelength to energy (Planck's law), it follows that

$$\frac{\Delta\lambda}{\lambda_{spr}} \approx \frac{\Delta E}{E_{spr}} \tag{2}$$

where $\Delta\lambda$ and ΔE are the shift caused by the refractive index change, in wavelength and energy units, respectively. λ_{spr} and E_{spr} are the SPR peak position in wavelength and energy units, respectively. Noting that $E_{spr} = hc/\lambda_{spr}$, where h is Planck's constant and c is the speed of light, yields

$$\Delta\lambda = \frac{\Delta E}{hc}\lambda_{spr}^{\ 2} \tag{3}$$

where ΔE is 0.14 eV for the air-hexane media change. Accordingly, for highly coupled arrays where λ_{spr} is relatively big, the $\Delta\lambda$ observed is much larger than that observed in noncoupled arrays (where λ_{spr} is relatively small) due to the λ_{spr}^2 dependence. In the Ag nanoparticle ensembles, the ability to tune the SPR wavelength to longer wavelengths via coupling interactions allows the same refractive index effect (0.14 eV) to be manifested as a bigger change in wavelength and this is the means of enhanced sensitivity.

The effect of near-field coupling between neighboring nanoparticles demonstrates that coupled nanoparticle geometries constitute more sensitive sensor platforms than those based on collections of isolated nanoparticles. Whereas near-field enhancement is actively exploited in surface enhanced Raman spectroscopy (SERS), the utilization of such effects to advantage in SPR-based spectroscopy has been minimal. Although experimental demonstration of the effect was reported a few years ago,[10] since that time development has been minimal with most relevant papers focusing on the effect of interparticle coupling on the optical properties of metal nanoparticles themselves.[1,2,12,13,29,30] As Jain and El-Sayed point out, the enhanced sensitivity to changes in the medium refractive index, caused by interparticle coupling effects, has been largely overlooked. In light of the magnitude of the effect, now confirmed experimentally by us and suggested by recent findings of the Quidant group,[11] it is clear that the design of assemblies of nanoparticles arranged to best exploit the near-field effect is a fruitful avenue of research in SPR-based spectroscopies. The fact that we observe these effects in assemblies of nanoparticles demonstrates that the effect is not strictly limited to dimers, as has been suggested,[9] and arrangements of nanoparticles that manifest strong interparticle coupling, and near-fields, are the critical factor for the enhancement effect. Having demonstrated that the enhancement is also operative in two-dimensional assemblies of nanoparticles opens up many possible geometric arrangements of nanoparticles as potential sensor elements tailored to exploit the enhanced sensitivity gained from interparticle coupling.

Conclusions

This work has demonstrated the ability to enhance the sensitivity of nanoparticle SPR peak positions to changes in the surrounding media by controlling the interparticle coupling interaction. The effect is another example of the advantages offered by controlling nanoarchitectures to nanometer precision. Changing the interparticle separation is critical to defining the nature of the interparticle coupling. For the 3.0 ± 0.5 nm diameter Ag nanoparticles, dipolar coupling is only dominant at distances greater than 50 nm. At distances less than 25 nm, wave function overlap is the dominant contributor to the coupling. Tuning the spacing between nanoparticles with nanometer precision within this range is required to observe the transition between coupling mechanisms. Regardless of mechanism, the results of this work show that the interparticle coupling energy is remarkably insensitive to changes in the medium. Similarly, the refractive index effect (0.14 eV) is found to be insensitive to changes in coupling. In the Ag nanoparticle ensembles considered, the ability to tune the SPR wavelength to longer wavelengths via coupling interactions allows this 0.14 eV refractive index effect to be manifested as a bigger change in wavelength and this is the means of enhanced sensitivity. In addition to substantiating the theoretical predictions, by establishing the source of the enhancement effect these results also demonstrate that the effect is not dimer-specific and any geometrical arrangement of nanoparticles resulting in strong interparticle coupling interactions will yield enhanced sensing capability.

References and Notes

(1) Atay, T.; Song, J.-H.; Nurmikko, A. *Nano Lett.* **2004**, *4*, 1627–1631.
(2) Su, K. X.; Wei, Q. H.; Zhang, X.; Mock, J. J.; Smith, D. R.; Schultz, S. *Nano Lett.* **2003**, *3*, 1087–1090.
(3) Pedersen, D. B.; Wang, S. *J. Phys. Chem. C* **2009**, *113*, 4797–4803.
(4) Kelly, K. L.; Lazarides, A. A.; Schatz, G. C. *Comput. Sci. Eng.* **2001**, *3*, 67–73.
(5) Zhao, L.; Kelly, K. L.; Schatz, G. C. *J. Phys. Chem. B* **2003**, *107*, 7343–7350.
(6) Hao, E.; Schatz, G. C. *J. Chem. Phys.* **2004**, *120*, 357–367.
(7) Jensen, T. R.; Duval, M. L.; Kelly, K. L.; Lazarides, A. A.; Schatz, G. C.; Van Duyne, R. P. *J. Phys. Chem. B* **1999**, *103*, 9846–9853.
(8) Haynes, C.; McFarland, A.; Zhao, L.; Van Duyne, R.; Schatz, G.; Gunnarsson, L.; Prikulis, J.; Kasemo, B.; Kall, M. *J. Phys. Chem. B* **2003**, *107*, 7337–7342.
(9) Jain, P. K.; El-Sayed, M. A. *Nano Lett.* **2008**, *8*, 4347–4352.
(10) Enoch, S.; Quidant, R.; Badeness, G. *Opt. Express* **2004**, *12*, 3422–3427.
(11) Aimovi, S. S.; Kreuzer, M. P.; Gonzalez, M. U.; Quidant, R. *ACS Nano* **2009**, *3*, 1231–1237.
(12) Pedersen, D. B.; Wang, S. *J. Phys. Chem. C* **2007**, *111*, 17493–17499.
(13) Pedersen, D. B.; Wang, S.; Paige, M.; Leontowich, A. *J. Phys. Chem. C.* **2007**, *111*, 5592–5598.
(14) Pedersen, D. B.; Wang, S. *J. Phys. Chem. C* **2007**, *111*, 1261–1267.
(15) Maier, S. A.; Brongersma, M. L.; Kik, P. G.; Atwater, H. A. *Phys. Rev. B* **2002**, *65*, 193408−1193408−4.
(16) Wei, Q. H.; Su, K. H.; Durant, S.; Zhang, X. *Nano Lett.* **2004**, *4*, 1067–1071.
(17) Zou, S.; Schatz, G. C. *J. Chem. Phys.* **2004**, *121*, 12606–12612.
(18) Hutter, E.; Fendler, J. H.; Roy, D. *J. Phys. Chem. B* **2001**, *105*, 11159–11168.

(19) Schatz, G. C.; Van Duyne, R. P. Electromagnetic Mechanism of Surface-enhanced Spectroscopy. In *Handbook of Vibrational Spectroscopy*; Chalmers, J. M. Griffiths, P. R., Eds.; John Wiley & Sons Ltd.: Chichester, U.K., 2002.

(20) Saini, S.; Srinivas, G.; Bagchi, B. *J. Phys. Chem. B* **2009**, *113*, 1817–1832.

(21) Dexter, D. L. *J. Chem. Phys.* **1953**, *21*, 836–850.

(22) Singh, H.; Bagchi, B. *Curr. Sci.* **2005**, *89*, 1710–1719.

(23) Wei, A. In *Nanoparticles: Nanostructure Science and Technology (Building Blocks for Nanotechnology Series)*; Rotello, V., Ed.; Plenum Publishing Corporation: New York, 2004; Chapter Plasmonic Nanomaterials: Enhanced Optical Properties from Metals Nanoparticles and their Ensembles, pp 173−199.

(24) Kamat, P. V. *J. Phys. Chem. B* **2002**, *106*, 7728.

(25) Pedersen, D. B.; Wang, S.; Duncan, E. J. S.; Liang, S. H. *J. Phys. Chem. C* **2007**, *111*, 13665–13672.

(26) Draine, B. T.; Flatau, P. J. *J. Opt. Soc. Am. A* **1994**, *11*, 1491–1499.

(27) Flatau, P.; Draine, B. T. *Opt. Lett.* **1997**, *22*, 1205–1207.

(28) Johnson, P. B.; Christy, R. W. *Phys. Rev. B* **1972**, *6*, 4370–4379.

(29) Bouhelier, A.; Bachelot, R.; Im, J.; Wiederrecht, G.; Lerondel, G.; Kostcheev, S.; Royer, P. *J. Phys. Chem. B* **2005**, *109*, 3195–3198.

(30) Rechberger, W.; Hohenau, A.; Leitner, A.; Krenn, J. R.; Lamprecht, B.; Aussenegg, F. R. *Opt. Commun.* **2003**, *220*, 137–141.

JP907991W